JOURNAL OF VIROLOGY, Apr. 2006, p. 3259–3272 Vol. 80, No. 7
0022-538X/06/$08.00+0 doi:10.1128/JVI.80.7.3259–3272.2006

Modulation of Poliovirus Replicative Fitness in HeLa Cells by Deoptimization of Synonymous Codon Usage in the Capsid Region

Cara Carthel Burns,* Jing Shaw, Ray Campagnoli, Jaume Jorba, Annelet Vincent, Jacqueline Quay,† and Olen Kew

Division of Viral and Rickettsial Diseases, National Center for Infectious Diseases, Centers for Disease Control and Prevention, Atlanta, Georgia 30333

Received 20 September 2005/Accepted 2 January 2006

We replaced degenerate codons for nine amino acids within the capsid region of the Sabin type 2 oral poliovirus vaccine strain with corresponding nonpreferred synonymous codons. Codon replacements were introduced into four contiguous intervals spanning 97% of the capsid region. In the capsid region of the most highly modified virus construct, the effective number of codons used (N_c) fell from 56.2 to 29.8, the number of CG dinucleotides rose from 97 to 302, and the G+C content increased from 48.4% to 56.4%. Replicative fitness in HeLa cells, measured by plaque areas and virus yields in single-step growth experiments, decreased in proportion to the number of replacement codons. Plaque areas decreased over an ~10-fold range, and virus yields decreased over an ~65-fold range. Perhaps unexpectedly, the synthesis and processing of viral proteins appeared to be largely unaltered by the restriction in codon usage. In contrast, total yields of viral RNA in infected cells were reduced ~3-fold and specific infectivities of purified virions (measured by particle/PFU ratios) decreased ~18-fold in the most highly modified virus. The replicative fitness of both codon replacement viruses and unmodified viruses increased with the passage number in HeLa cells. After 25 serial passages (~50 replication cycles), most codon replacements were retained, and the relative fitness of the modified viruses remained well below that of the unmodified virus. The increased replicative fitness of high-passage modified virus was associated with the elimination of several CG dinucleotides. Potential applications for the systematic modulation of poliovirus replicative fitness by deoptimization of codon usage are discussed.

The use of synonymous codons at unequal frequencies, the codon usage bias, is characteristic of all biological systems (26, 27). The strength and direction of codon usage bias are related to the genomic G+C content and the relative abundance of different isoaccepting tRNAs (reviewed in references 1, 16, and 53). Codon usage can affect the efficiency of gene expression. In bacteria (*Escherichia coli*) (26, 75), yeast (*Saccharomyces cerevisiae*) (5, 27), plants (*Arabidopsis thaliana*) (12), nematodes (*Caenorhabditis elegans*) (16), and insects (*Drosophila melanogaster*) (50), the most highly expressed genes use codons matched to the most abundant tRNAs (2). In contrast, in humans and other vertebrates, codon usage bias is much more strongly correlated with the G+C content of the isochore where the gene is located (51, 71) than with the breadth or level of gene expression (16) or the number of corresponding tRNA genes (28, 30). Despite the weak correlation between codon usage and the levels of gene expression in mammalian cells (16, 71), imbalances between codon usage and tRNA abundance can sharply reduce the levels of gene expression.

Optimization of codon composition is frequently required for the efficient expression of genes in heterologous host systems (3, 31, 67, 76). For example, the expression of human immunodeficiency virus type 1 gp120 in mammalian cells (3) and *Plasmodium falciparum* surface antigens in *Pichia pastoris* (76) is enhanced by replacing the natural codons with preferred codons of the most highly expressed genes of the expression system. Conversely, replacement of the natural codons with nonpreferred codons can dramatically decrease the efficiency of gene expression in *E. coli* (60), *S. cerevisiae* (23), *D. melanogaster* (10), and mammalian cells (81).

Codon usage bias in human RNA viruses generally appears to be low, and differences in codon usage are most strongly correlated with the genomic G+C content (29), which ranges from ~35% in rotavirus (17) to ~70% in rubella virus (15). Codon usage in vertebrate genomic DNAs and most eukaryotic RNA viruses is also shaped by the suppression of CG dinucleotides (33). Polioviruses and the closely related species C human enteroviruses have moderate and similar (43% to 47%) G+C contents in their RNA genomes (8), apparently low codon usage biases (29), and low abundances of CG dinucleotides (33, 57, 61, 70).

We have studied the effects of altered codon composition on the replicative fitness of poliovirus. Nucleotide substitution in poliovirus genomes is both highly dynamic and remarkably conservative. The overall rate of nucleotide substitution exceeds 1% per site per year, and because the large majority (~90% in the capsid region) of substitutions generate synonymous codons, substitution rates at sites of codon degeneracy are over 3% per synonymous site per year (19, 43, 45, 77). Despite the exceptionally high rate of turnover of synonymous

* Corresponding author. Mailing address: Respiratory and Enteric Viruses Branch, G-10, Division of Viral and Rickettsial Diseases, National Center for Infectious Diseases, Centers for Disease Control and Prevention, 1600 Clifton Rd., N.E., Atlanta, GA 30333. Phone: (404) 639-5499. Fax: (404) 639-4011. E-mail: cburns@cdc.gov.

† Present address: Office of Technology Development, The University of North Carolina at Chapel Hill, Chapel Hill, NC 27599.

codons, poliovirus codon usage is stable across poliovirus genotypes and serotypes (70).

In this study, we deoptimized codon usage in the Sabin type 2 (Sabin 2) oral poliovirus vaccine (OPV) strain (59, 64, 70) by replacing the natural codons in the capsid region with synonymous nonpreferred (minor) codons. Virus plaque sizes and yields in cell culture decreased in proportion to the number of nonpreferred codons incorporated into the capsid region sequences. The altered codon compositions were largely conserved during 25 serial passages in HeLa cells. The fitness for replication in HeLa cells of both the unmodified Sabin 2 virus and the codon replacement viruses increased with higher passage numbers; however, the relative fitness of the modified viruses remained lower than that of the unmodified virus. In contrast to expectations, the major change in capsid codon usage did not substantially alter the synthesis and processing of viral proteins in infected cells. When the most highly modified virus construct was compared to the unmodified construct, the yield of viral RNA in infected cells decreased ~3-fold, while the particle/PFU ratio increased ~18-fold. The potential application of codon usage deoptimization to the systematic development of improved attenuated RNA virus vaccines having well-defined levels of replicative fitness and enhanced genetic stabilities is discussed below.

MATERIALS AND METHODS

Virus and cells. The Sabin Original +2 (64) master seed of the Sabin type 2 OPV strain (P712 Ch 2ab) was kindly provided by R. Mauler of Behringwerke AG (Marburg, Germany). The virus was grown at 35°C in suspension cultures (63) of HeLa S3 cells (human cervical carcinoma cells; ATCC CCL-2.2) (11) or in monolayer cultures of HeLa (ATCC CCL-2) (11) or RD (human rhabdomyosarcoma cells; ATCC CCL-136) cells. Some initial plaque assays were performed with HEp-2C cells (11).

Preparation of infectious Sabin 2 clones. Poliovirus RNA was extracted from 250 μl of cell culture lysate (from ~75,000 infected cells) by using TRIZOL LS reagent (Invitrogen, Carlsbad, Calif.) and further purified on Centri-Sep columns (Princeton Separations, Adelphia, N.J.). Full-length cDNA was prepared by reverse transcription (42°C for 2 h) of ~1 μg of viral RNA in a 20-μl reaction mix containing a 500 μM concentration of each deoxynucleoside triphosphate (dNTP; Roche Applied Science, Indianapolis, Ind.), 200 U Superscript II reverse transcriptase (Invitrogen), 40 U RNase inhibitor (Roche), 10 mM dithiothreitol, and 500 ng primer S2-7439A-B [CCTAAGC$(T)_{30}$CCCCGAATTAAAGAAAAATTTACCCCTACA] (13) in Superscript II buffer. After reverse transcription, 2 U RNase H (Roche) was added and incubated at 37°C for 40 min. Long-PCR amplification of viral cDNA was performed using TaqPlus Precision (Stratagene, La Jolla, Calif.) and AmpliWax PCR Gem 100 beads (Applied Biosystems, Foster City, Calif.) for "hot start" PCR in thin-walled tubes. The bottom mix (50 μl) contained a 400 μM concentration of each dNTP (Roche) and 250 ng each of primers S2-7439A-B and S2-1S-C (GTAGTCGACTAATACGACTCACTATAGGTTAAAACAGCTCTGGGGTTG) in TaqPlus Precision buffer. A wax bead was added to each tube, and samples were heated at 75°C for 4 min and cooled to room temperature. The top mix (50 μl) contained 2 μl of cDNA and 10 U TaqPlus Precision in TaqPlus Precision buffer. The samples were incubated in a thermal cycler at 94°C for 1 min and then amplified by 30 PCR cycles (94°C for 30 s, 60°C for 30 s, and 72°C for 8 min), followed by a final denaturation step of 94°C for 1 min and a final extension step of 72°C for 20 min.

PCR products were purified using a QIAquick PCR purification kit (QIAGEN, Valencia, Calif.) and sequentially digested for 2 h at 37°C with the restriction enzymes SalI and HindIII prior to gel purification. PCR products were ligated into pUC19 plasmids following standard methods (65), and ligated plasmids were transformed into XL-10 Gold supercompetent *E. coli* cells (Stratagene) (65). Sequences of the inserts were determined by cycle sequencing using an automated DNA sequencer (Applied Biosystems) (43).

Virus preparation. Full-length cDNA plasmids were linearized with HindIII and purified on QIAquick columns prior to RNA transcription from 1 μg of plasmid DNA using a Megascript T7 in vitro transcription kit (Ambion, Austin, Tex.). RNA yields were estimated by using DNA Dipsticks (Invitrogen), and RNA chain lengths were analyzed by electrophoresis on 1% agarose-2.2 M formaldehyde gels (40) prior to transfection. RD cells were transfected with transcripts of viral RNA by using Tfx-20 reagent (Promega, Madison, Wis.). Briefly, semiconfluent RD cells in 12-well cell culture plates were inoculated with 500 μl minimum essential medium (incomplete MEM) (GIBCO, Carlsbad, Calif.) containing 0.1 μg viral RNA transcript and 0.45 μl Tfx-20 reagent. Plates were incubated for 1 h at 35°C prior to the addition of 1.5 ml complete MEM (incomplete MEM supplemented with 100 U/ml penicillin, 100 μg/ml streptomycin, 2 mM L-glutamine, 0.075% $NaHCO_3$, and 10 mM HEPES [pH 7.5]) (GIBCO) containing 3% fetal bovine serum (FBS; HyClone, Logan, Utah). Negative controls were performed using RNA transcribed from pBluescript II SK(+) (Stratagene) containing a cDNA insert of the incomplete viral genome (truncated at base 7200 by digestion with BamHI) in reverse orientation from a T3 promoter. A complete cytopathic effect (CPE) was observed for most viruses after incubation at 35°C for 18 to 20 h, at which time 400 μl from each transfected well was transferred to a confluent RD cell monolayer in a 75-cm^2 flask containing complete MEM. In this second passage, complete CPE was observed after 24 h at 35°C for all but the most highly modified viruses (e.g., S2R23), which were incubated for an additional 24 to 48 h. Viruses were liberated from the infected cells by three freeze-thaw cycles and clarification by centrifugation (15,000 × *g*, 15 min). The sequences of all virus stocks were verified by in vitro amplification of two large overlapping fragments and sequence analysis of the PCR products.

Site-directed mutagenesis. Single base substitutions were introduced by using a QuikChange site-directed mutagenesis kit (Stratagene). Briefly, two complementary primers containing the desired mutation were designed for PCR amplification of the plasmid containing the Sabin 2 cDNA insert. Amplification was performed using *Pfu* Turbo DNA polymerase on 5 ng of template DNA for 15 cycles at 95°C for 30 s, 50°C for 1 min, and 68°C for 15 min. PCR products were digested for 1 h at 37°C with 10 U of DpnI prior to transformation into XL-1 Blue supercompetent *E. coli* cells. Colonies were grown and screened by sequencing as described above.

Construction of recombinant cDNA plasmids by assembly PCR and exchange of mutagenesis cassettes. Multiple base substitutions were introduced by assembly PCR (68). Primers were designed to span the region of interest, with complementary 40-mers overlapping by 10 nucleotides (nt) on each end. A first round of assembly (30 PCR cycles of 94°C for 45 s, 52°C for 45 s, and 72°C for 45 s) was performed with a 20-μl reaction mixture containing TaqPlus Precision buffer, 10 U TaqPlus Precision, 5 pmol of each primer, and a 200 μM concentration of each dNTP. A second round of assembly (25 PCR cycles of 94°C for 45 s, 50°C for 45 s, and 72°C for 2 min) was performed, using the outermost sense and antisense primers in a 100-μl reaction mixture containing TaqPlus Precision buffer, 2 μl of product from the first assembly round, 10 U TaqPlus Precision, 15 pmol of each primer, and a 400 μM concentration of each dNTP. PCR products were purified on QIAquick PCR columns prior to digestion, ligation, and transformation into XL-10 Gold supercompetent cells. Clones were grown and screened by sequencing of the insert as described above.

The sequence of our full-length Sabin 2 infectious cDNA construct, S2R9, differed from the published sequence of a reference Sabin 2 strain (59) at three synonymous third codon positions, i.e., G_{2616} (in the VP1 region; A was replaced to introduce an EagI restriction site), T_{3303} (in the VP1 region; A was replaced to introduce an XhoI site), and A_{5640} (in the $3C^{pro}$ region). The virus derived from the S2R9 construct was used as our reference Sabin 2 strain. Recombinant cDNAs having different combinations of blocks of replacement codons were constructed using standard methods (37).

Plaque assay. Plaque assays were performed by a modification of previously described methods (78). Briefly, confluent HeLa (or HEp-2C) cell monolayers in 57-cm^2 cell culture dishes were washed, inoculated with virus in incomplete MEM, and incubated at room temperature for 30 min prior to the addition of 0.45% SeaKem LE agarose (BioWhittaker Molecular, Rockland, Maine) in complete MEM containing 2% fetal bovine serum (FBS). Plates were incubated for 60 h at 35°C, fixed with 0.4% formaldehyde, and stained with 3% crystal violet. Plaque sizes were quantified from digital images of the plates made with a FOTO/Analyst archiver system (Fotodyne, Hartland, Wis.) and by subsequent image analysis using Scion Image for Windows (Scion Corp., Frederick, Md.).

Cell culture infectivity assay. Virus infectivities were also measured by the limiting dilution method, using HeLa (or RD) cell monolayers cultured in 96-well plates. Plates were monitored for CPE for up to 7 days, and 50% cell culture infectious dose ($CCID_{50}$) titers were calculated by the method of Kärber (32).

Single-step growth curves. HeLa S3 suspension cells (1×10^7 cells in 2.5 ml) were infected at a multiplicity of infection (MOI) of 5 PFU/cell, with stirring, for 30 min at 25°C. Cells were then sedimented by low-speed centrifugation and resuspended in 2.5 ml warm complete medium (MEM lacking calcium salts)

containing glutamine, 5% FBS, penicillin-streptomycin, and 25 mM HEPES (pH 7.5). Incubation was continued at 35°C in a water bath, with orbital shaking at 300 rpm. Samples were withdrawn at 2-h intervals from 0 to 14 h postinfection and titrated by plaque assay at 35°C.

Preparation of radiolabeled viral proteins in infected HeLa cells. Confluent HeLa cell monolayers (~1.6×10^6 cells per 9.5-cm^2 well; six-well plates) were infected with virus derived from the S2R9, S2R19, or S2R23 cDNA construct at an MOI of 25 PFU/cell and incubated at 35°C for 4 h in a 5% CO_2 incubator in 2.0 ml complete MEM with 2% FBS. The medium was replaced with 1.9 ml of labeling medium (200 μCi [^{35}S]methionine in a 1:7 mixture of complete MEM and MEM without methionine, supplemented with 2% FCS). Cultures were incubated in a CO_2 incubator at 35°C for 3 h. The radioactive medium was removed, and cells were rinsed twice with phosphate-buffered saline. Cells were lysed in 1 ml lysis buffer (1% NP-40 in 10 mM NaCl, 10 mM Tris-Cl [pH 7.5], and 1.5 mM $MgCl_2$) at 35°C for 1 min (6). Lysates were transferred to microcentrifuge tubes on ice and centrifuged at 2,000 × *g* for 2 min at 4°C, and the supernatants were transferred to new tubes. Sodium dodecyl sulfate (SDS) was added to the supernatants to a final concentration of 1%, and samples were frozen. Labeled viral proteins were separated by SDS-10% polyacrylamide gel electrophoresis (SDS-10% PAGE) (38). Gels were fixed, washed, dried, and exposed to Kodak BioMax film for 1 to 3 days at room temperature.

In vitro translation. Viral RNAs transcribed from recombinant plasmids were translated in vitro in nuclease-treated rabbit reticulocyte lysates (Promega) supplemented with uninfected HeLa cell extracts as previously described (6, 7, 80). Briefly, 35 μl micrococcal nuclease-treated, supplemented rabbit reticulocyte lysate was mixed with 7 μl HeLa cell extract, 1 μl 1 mM amino acid mix (without methionine), various amounts of RNA (0.2 μg to 1 μg), 30 μCi [^{35}S]methionine (1,200 Ci/mmol), and 40 U Protector RNase inhibitor (Roche) in a final volume of 50 μl. The reaction mixtures were incubated at 30°C for 3 h. Samples were analyzed by SDS-10% PAGE as described above.

Preparation of purified virions. Viruses were propagated in RD cells, liberated by freeze-thawing, and concentrated by precipitation with polyethylene glycol 6000 (52). Virions were purified by pelleting, isopycnic centrifugation in CsCl, and repelleting, essentially as described previously (52). The number of virus particles in each preparation recovered from the CsCl band with a buoyant density of 1.34 g/ml was calculated from the absorbance at 260 nm, using the relationship of 9.4×10^{12} virions per optical density unit at 260 nm (62).

Measurement of viral RNAs in infected cells. The production of viral RNAs in infected HeLa cells during the single-step growth experiments described above was measured by quantitative reverse transcription-PCR using a Stratagene MX4000 PCR system programmed to incubate reaction mixtures at 48°C for 30 min and 95°C for 10 min, followed by 60 PCR cycles (95°C for 15 s, 60°C for 1 min). Sequences within the 3′ half of the 3D^{pol} region of Sabin 2 were amplified using primers S2/7284A (ATTGGCACACTCCTGATTTTAGC) and S2/7195S (CAAAGGATCCCAGAAACACACA), and the amplicon yield was measured by the fluorescence at 517 nm of the TaqMan probe S2/7246AB (TTCTTCTT CGCCGTTGTGCCAGG), with 6-carboxyfluorescein attached to the 5′ end and BHQ-1 (Biosearch Technologies, Novato, Calif.) attached to the 3′ end. Stoichiometric calculations used a value of 2.4×10^6 for the molecular weight of Sabin 2 RNA (36, 70).

Infectivities of RNA transcripts. Transcripts (0.1 μg) from constructs S2R9, S2R19, and S2R23 were transfected onto monolayers of 2.5×10^5 HeLa cells as described above for RD cells. After 12 h of incubation at 35°C, viruses were liberated by three freeze-thaw cycles, and the clarified supernatants were assayed for infectivity by the limiting dilution method on HeLa cell monolayers as described above.

Serial passage of recombinant virus in HeLa cells. Poliovirus constructs S2R9, S2R19, and S2R23 were passaged 25 times in HeLa cell monolayers in T75 flasks incubated at 35°C for 36 h, with input MOIs ranging from 0.1 to 0.4 PFU/cell (measured on HeLa cells). Every fifth passage, virus plaque areas, plaque yields, and the genomic sequences of the bulk virus populations were determined, and the MOI was readjusted to ~0.1 PFU/cell.

Analysis of RNA secondary structure. Predictions of the secondary structures of the RNA templates of virus constructs S2R9, S2R19, and S2R23 were performed using the mfold v. 3.1 program (47, 54, 82), which implements an energy minimization algorithm that finds a structure with the calculated minimum free energy (MinE). The MinE structure is plotted and color annotated with P-num values, which provide a measure of the number of alternative pairings for each nucleotide base (82). The running parameters were set to default values, except for the folding temperature (*T*), which was set to 35°C. Structures with suboptimal thermodynamic stabilities having increased free energy increments ($\Delta\Delta G_{35°C}$) of 4 kcal/mol, 8 kcal/mol, and 12 kcal/mol were analyzed by using color-annotated energy dot plots (82).

Nucleotide sequence accession numbers. Complete genomic sequences of the poliovirus constructs S2R9, S2R19, and S2R23 were submitted to the GenBank library under accession numbers DQ205099, DQ205098, and DQ205100, respectively.

RESULTS

Codon usage in poliovirus. Mononucleotide and dinucleotide frequencies and codon usage were analyzed in the original reports of poliovirus genomic sequences (36, 57, 61, 70). The mono-, di-, and trinucleotide frequency patterns are similar for the three Sabin strains (70) and appear to be conserved across poliovirus genotypes (24, 35, 39, 42, 46, 78) and other human enterovirus species C serotypes (8). As with other enteroviruses, the component bases in the Sabin 2 open reading frame (ORF) are present in approximately equal proportions (24.0% U, 22.9% C, 29.9% A, and 23.1% G) (59, 70), a property favorable to a low bias in codon usage (53). All codons are used in poliovirus ORFs (70), and the overall degree of codon usage bias is indeed low (29). One measure of codon usage bias is the effective number of codons used in a genetic interval (N_C), which can vary from 20 (only one codon used for each amino acid) to 61 (all codons used randomly) (74). The N_C values for Sabin 2 are 56.0 for the capsid region and 54.6 for the complete ORF. As with the genomes of vertebrates (34) and nearly all RNA viruses (33), the dinucleotide CG is suppressed in the Sabin 2 genome (70), and the observed pattern of codon usage reflects this suppression (Table 1).

Strategy for deoptimization of synonymous codon usage. Despite the low overall bias in codon usage in Sabin 2, some synonymous codons are used at much lower frequencies than others (Table 1). To examine the biological effects of altered codon usage, we replaced the original codons of Sabin 2 with synonymous nonpreferred codons (Table 1). The codon replacements were introduced only within the P1/capsid region sequences because those sequences uniquely identify poliovirus serotypes (8, 20, 42, 78), as P2/noncapsid region, P3/noncapsid region, 3′-untranslated region (3′-UTR), and 5′-UTR sequences are exchanged out by recombination with other species C enteroviruses during poliovirus circulation (8, 20, 35, 42, 78). Because the usage bias was very low for most twofold degenerate codons (except codons for His and Tyr), we replaced only sixfold, fourfold, and threefold degenerate codons. Synonymous codons for nine amino acids were replaced by single nonpreferred codons, as follows: CUU for Leu, AGC for Ser, CGG for Arg, CCG for Pro, GUC for Val, ACG for Thr, GCG for Ala, GGU for Gly, and AUC for Ile (Table 1). Whenever possible, we chose codons with G or C at degenerate positions in order to increase the G+C contents of the modified viral genomes.

Replacement codons were introduced into a full-length infectious cDNA clone derived from Sabin 2 (construct S2R9) within an interval (nt 748 to 3302) spanning all but the last 27 codons of the capsid region (Fig. 1). The capsid interval was divided into the following four mutagenesis cassettes: *A* (nt 657 to 1317; 661 bp), *B* (nt 1318 to 2102; 785 bp), *C* (nt 2103 to 2615; 513 bp), and *D* (nt 2616 to 3302; 687 bp) (Fig. 1). Mutagenesis cassette *A*, bounded by restriction sites BstZ17I and AvrII, includes the last 91 nucleotides of the 5′ UTR, but no 5′-UTR sequences were modified in cassette *A*. Within each

TABLE 1. Codon usage in codon replacement capsid interval and complete open reading frame in *ABCD*, *ABCd*, and *abcd* virus genomes

Amino acid	Codon[a]	Codon usage (no. of codons in sequence)					
		Capsid interval (nt 748 to 3303)			Complete ORF (nt 748 to 7368)		
		ABCD[b]	*ABCd*[c]	*abcd*[d]	*ABCD*[b]	*ABCd*[c]	*abcd*[d]
Arg	CGA	4	1	0	7	4	3
	CGC	11	7	0	13	9	2
	CGG	2	17	39	7	22	44
	CGU	0	0	0	3	3	3
	AGA	17	9	0	45	37	28
	AGG	5	5	0	23	23	18
Leu	CUA	7	6	1	33	32	27
	CUC	7	6	0	27	26	20
	CUG	14	10	0	25	21	11
	CUU	4	14	55	22	32	73
	UUA	9	9	1	25	25	17
	UUG	18	14	2	40	36	24
Ser	UCA	18	11	0	43	36	25
	UCC	14	11	2	33	30	21
	UCG	6	1	0	8	3	2
	UCU	8	7	0	19	18	11
	AGC	9	25	63	20	36	74
	AGU	10	10	0	26	26	16
Thr	ACA	20	17	0	47	44	27
	ACC	24	19	1	55	50	32
	ACG	11	23	74	17	29	80
	ACU	20	16	0	47	43	27
Pro	CCA	21	16	0	53	48	32
	CCC	19	15	0	32	28	13
	CCG	9	21	59	19	31	69
	CCU	12	9	2	18	15	8
Ala	GCA	23	16	0	61	54	38
	GCC	16	13	2	40	37	26
	GCG	10	26	66	17	33	73
	GCU	19	13	0	49	43	30
Gly	GGA	12	8	0	38	34	26
	GGC	8	7	0	30	29	22
	GGG	20	16	2	37	33	19
	GGU	14	23	52	42	51	80
Val	GUA	10	8	1	24	22	15
	GUC	10	27	55	21	38	66
	GUG	20	10	1	55	45	36
	GUU	17	12	0	40	35	23
Ile	AUA	16	12	0	30	26	14
	AUC	15	22	45	47	54	77
	AUU	14	11	0	59	56	45
Lys	AAA	13	13	13	64	64	64
	AAG	18	18	18	58	58	58
Asn	AAC	25	25	25	61	61	61
	AAU	25	25	25	52	52	52
Gln	CAA	18	18	18	47	47	47
	CAG	9	9	9	32	32	32
His	CAC	12	12	12	30	30	30
	CAU	6	6	6	19	19	19
Glu	GAA	16	16	16	57	57	57
	GAG	19	19	19	56	56	56
Asp	GAC	23	23	23	51	51	51
	GAU	19	19	19	62	62	62
Tyr	UAC	21	21	21	57	57	57
	UAU	16	16	16	43	43	43
Cys	UGC	10	10	10	20	20	20
	UGU	5	5	5	22	22	22
Phe	UUC	14	14	14	36	36	36
	UUU	21	21	21	48	48	48
Met	AUG	26	26	26	67	67	67
Trp	UGG	13	13	13	28	28	28

[a] Nonpreferred codons used as replacement codons are shown in boldface type.

[b] *ABCD* represents the virus construct S2R9, which differs from the reference Sabin 2 strain sequence at three synonymous third-position sites: $A_{2616}\rightarrow G$ (VP1 region), $A_{3303}\rightarrow T$ (VP1 region), and $T_{5640}\rightarrow A$ ($3C^{pro}$ region).

[c] *ABCd* represents the virus construct S2R19, which has replacement codons across an interval spanning 76% of the VP1 region.

[d] *abcd* represents the virus construct S2R23, which has replacement codons across an interval spanning 97% of the capsid region.

cassette, synonymous codons for the nine amino acids were comprehensively replaced, except at 15 positions (replacement at 11 of these positions would have eliminated desirable restriction sites or generated undesirable restriction sites). Unmodified cassettes are identified by capital italic letters; the corresponding cassettes with replacement codons are identified by lowercase italic letters. Thus, the reference Sabin 2 derivative (derived from cDNA construct S2R9) is identified as *ABCD*, and the fully modified virus (derived from cDNA construct S2R23) is identified as *abcd* (Fig. 2).

The modifications dramatically altered the mono-, di-, and trinucleotide (codon) frequencies in the capsid region (Tables 1 and 2). In the fully modified virus, *abcd*, nearly half (425/879; 48.4%) of the *ABCD* capsid region codons were replaced, and a total of 542 substitutions (90 at the first codon position, 44 at the second position, and 408 at the third position) were introduced into the 2,555 nucleotides of the codon replacement capsid region interval (Table 1). Compared with *ABCD*, the N_C value for the capsid region of *abcd* fell from 56.2 to 29.8, the number of CG dinucleotides rose from 97 to 302, and the %G+C increased from 48.4% to 56.4% (Table 2). These changes were nearly uniformly distributed over the codon replacement capsid region interval (Fig. 1; Table 2).

Growth properties of codon replacement viruses. RNA transcripts of cDNA constructs with various combinations of codon replacement cassettes (Fig. 2) were transfected into RD cells. The viruses obtained from the primary transfections were passaged again in RD cells to increase virus titers. The growth properties of the viruses were then measured in HeLa cells by plaque assays (Fig. 3) and single-step growth experiments (Fig. 4).

(i) Plaque assays. An approximately linear inverse relationship was observed between the mean plaque area in HeLa cells and the number of nucleotide changes introduced into the capsid region (Fig. 3A and C). Similar inverse linear relationships were observed when the abscissa was rescaled to the number of replacement codons or to the number of CG dinucleotides (data not shown). There was no strong polarity for the effects of codon replacement within the capsid region, as the introduction of replacement codons into any combination of the four cassettes reduced plaque areas approximately in proportion to the total number of replacement codons. However, replacements of codons in the VP1 region (cassette *D*) appeared to have stronger effects than replacements elsewhere (Fig. 3). Codon replacement in three or four cassettes generally conferred a minute plaque phenotype (mean plaque area of <25% that of the unmutagenized *ABCD* prototype), and the mean areas of the observed plaques of the *abcd* virus were ~9% those of the *ABCD* prototype (Fig. 3). An exception was virus *abcD*, which had a greater mean plaque area (~38% that of *ABCD*) than *Abcd*, *aBcd*, and *abCd*, underscoring the stronger influence on plaque size of codon replacement within the VP1 region.

Measurements of plaque areas and total plaque numbers became increasingly difficult as plaque sizes decreased. The diameters of poliovirus plaques are typically heterogeneous, and this heterogeneity was observed with the plaques of all virus constructs. Precise measurement was most difficult with the smallest of the minute plaques, as was discriminating very minute plaques from other small defects in the cell monolayers. Extended incubation of plaque cultures to 72 h increased

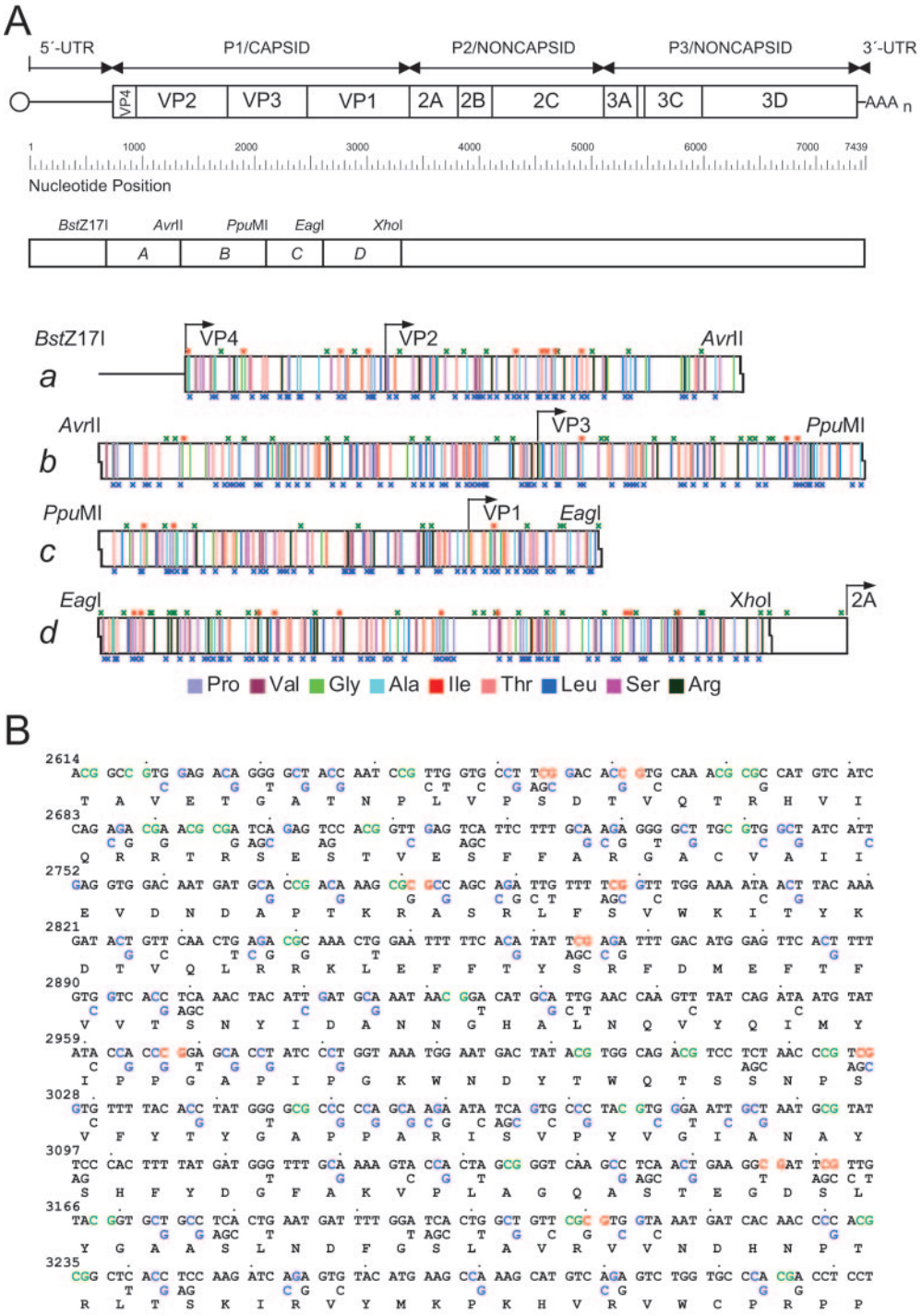

FIG. 1. (A) Locations of codon replacement cassettes *A* to *D* in the infectious Sabin 2 (S2R9) full-length cDNA clone. In the schematic of the poliovirus genome (top), the single ORF is represented by an open rectangle flanked by the 5′ and 3′ UTRs, represented by lines. The locations along the genome of cassettes *A* to *D* and of the restriction sites used for construction of the codon replacement cDNAs are shown in the rectangle (middle). In the blocks representing codon replacement cassettes *a* to *d* (bottom), colored bars show positions of codon deoptimization. The locations of CG dinucleotides are indicated by x's above (green, originally present and retained during codon replacement; red, originally present and lost during codon replacement) and below (blue, generated by codon replacement) the cassette blocks. (B) Replacement codons of cassette *D*. Original S2R9 Sabin 2 triplets (top of each alignment) are aligned with the codon replacement residues (middle) and the shared deduced amino acids for both the *D* and *d* cassettes (bottom). Original CG dinucleotides are shown in green, new CG dinucleotides are shown in blue, and CG dinucleotides lost during codon replacement are shown in red.

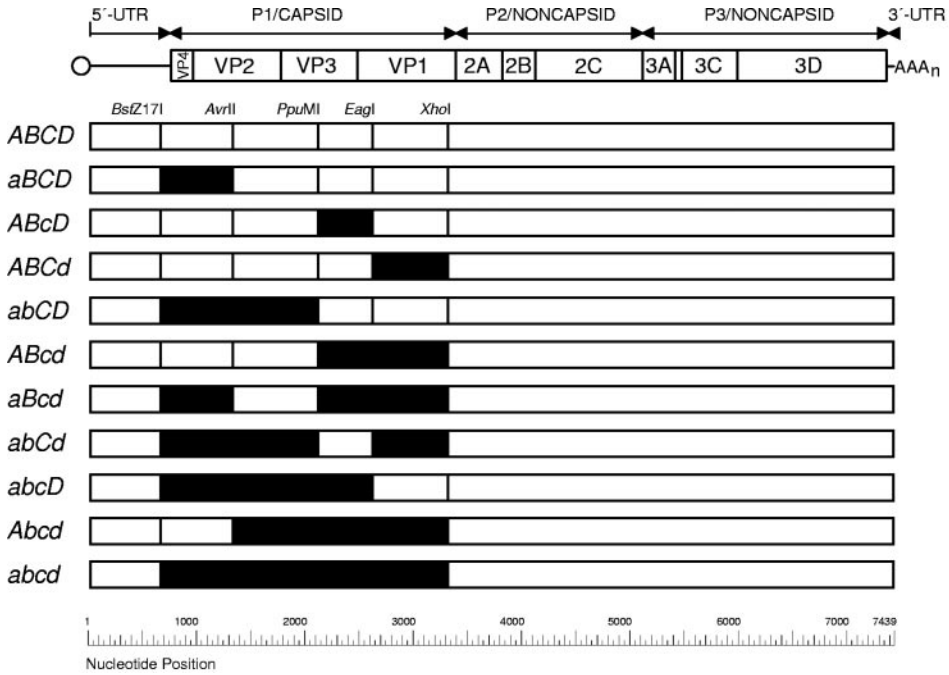

FIG. 2. Sabin 2 codon replacement constructs aligned with a schematic of the poliovirus genome. White rectangles indicate unmodified cassettes (identified by capital letters), and black rectangles indicate cassettes with replacement codons (identified by lowercase letters).

plaque diameters but did not increase the plaque counts. Plaque morphologies were similar when the plaque assays were performed on HEp-2C cells, but the titers were ~2.5-fold lower than the HeLa plaque titers for all virus constructs.

(ii) Single-step growth experiments. A plaque is the result of several cycles of replication, such that any differences in replication rates are amplified. To examine the relationships between plaque size, virus growth rate, and virus yield, single-step growth experiments (input MOI, 5 PFU/cell) were performed with HeLa cells at 35°C, and virus titers were determined by plaque assay on HEp-2C cells (35°C), which generally had more uniform monolayers, facilitating the enumeration of minute plaques. Mean virus yields from the single-step growth experiments generally decreased as the number of replacement codons increased (Fig. 3B and 4). Mean virus yields were highest (5.2×10^8 PFU/ml [equivalent to ~130 PFU/cell] for HEp-2C cells) for the *ABCD* prototype and viruses *ABcD* and *aBCD*. Yields were 4- to 8-fold lower with *ABCd*, *abCD*, and *ABcd*, 12- to 24-fold lower with *abcD* and *aBcd*, 30- to 45-fold lower with *Abcd* and *abCd*, and ~65-fold lower (8.3×10^6 PFU/ml; ~2 PFU/cell) with *abcd* (Fig. 3B and 4). Moreover, the production of infectious virus appeared to be slower in the codon replacement viruses than in the unmodified *ABCD* prototype. Although maximum plaque yields were obtained at 10

TABLE 2. Effective numbers of codons used, numbers of CG dinucleotides, and G+C contents in codon replacement capsid region sequences

Construct[a]	Length of codon replacement interval (bp)	N_C[b]			No. of CG dinucleotides[c]			%G+C		
		Replacement interval (orig/mod)[d]	Complete capsid region[e]	Complete ORF	Replacement interval (orig/mod)[d]	Complete capsid region[e]	Complete ORF	Replacement interval (orig/mod)[d]	Complete capsid region[e]	Complete ORF
ABCD[f,g]	—	56.0/—	56.2	54.6	94/—	97	181	48.5/—	48.4	46.0
aBCD	570[h]	57.3/30.8	56.1	56.4	20/63	140	224	48.1/56.0	50.1	46.7
AbCD	785	56.0/29.9	53.1	55.7	25/89	161	245	48.4/56.1	50.7	47.0
ABcD	513	57.7/28.2	56.3	56.0	13/59	143	227	48.3/57.0	50.1	46.7
ABCd	687	54.0/28.4	54.6	56.5	36/88	149	233	49.1/57.7	50.7	46.5
abcd	2555	56.0/29.3	29.8	47.3	94/299	302	386	48.5/56.7	56.4	49.2

[a] Constructs correspond to the following infectious cDNA plasmids, clones, and virus derivatives: *ABCD*, S2R9; *aBCD*, S2R28; *AbCD*, not constructed; *ABcD*, S2R20; *ABCd*, S2R19; and *abcd*, S2R23. The N_C values, numbers of CG dinucleotides, and %G+C for all other constructs can be calculated from the table.
[b] Effective number of codons used (74). One replacement codon spanned the EagI restriction cleavage site and was counted as part of cassette *D*.
[c] One CG dinucleotide spanned the EagI restriction cleavage site and was counted as part of cassette *D*.
[d] Orig/mod, original construct/modified codon replacement construct.
[e] The complete capsid region is nt 748 to 3384.
[f] The S2R9 (*ABCD*) sequence differs from the reference Sabin 2 sequence at three synonymous third-position sites (see Table 1).
[g] —, unmodified.
[h] Does not include the 3′-terminal 91 bases of the 5′ UTR at the 5′ end of cassette *A* (nt 657 to 747) that were not modified.

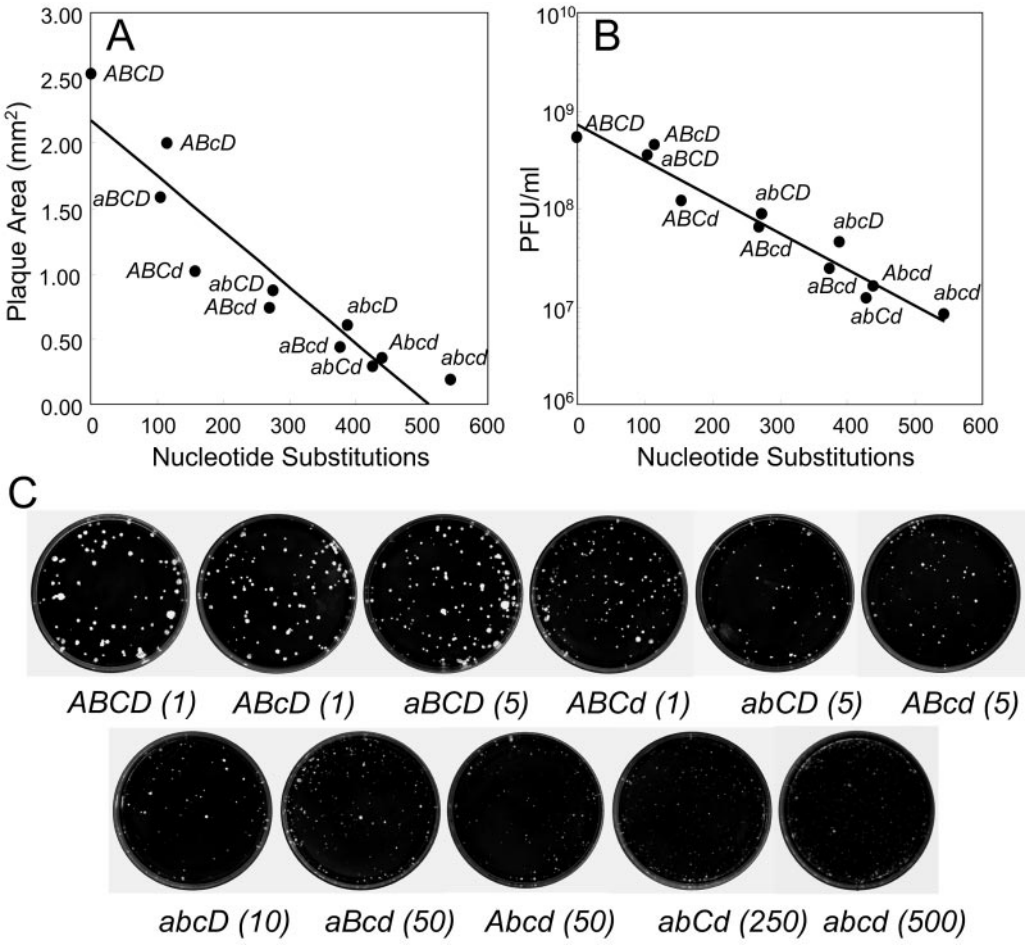

FIG. 3. (A) Mean plaque areas on HeLa cells versus numbers of nucleotide substitutions in the capsid region. Mean plaque areas were determined for plaques on HeLa cell monolayers after incubation at 35°C for 60 h. The coefficient of determination (R^2) for the regression line was 0.88. (B) Virus yields (at 12 h postinfection) in a single-step growth experiment with HeLa S3 cells versus numbers of nucleotide substitutions in the capsid region. Plaque assays (35°C, 72 h) were performed on HEp-2C cells. Plaque morphologies were similar for HEp-2C and HeLa cell monolayers, but plaque yields were ~2.5-fold lower on HEp-2C cells. The coefficient of determination (R^2) for the regression line was 0.94. (C) Plaque morphologies on HeLa cells (35°C, 60 h). Numbers in parentheses indicate relative amounts of infected cell culture lysates yielding the plaques shown in the dishes.

to 12 h for all viruses, the proportions of the final yields detected at 4 h were lower for the codon replacement viruses (Fig. 4).

Synthesis of viral proteins in infected HeLa cells. Our working hypothesis was that the replacement of preferred codons with nonpreferred codons might lower replicative fitness primarily by reducing the rate of translation (at the level of polypeptide chain elongation) of viral proteins and potentially disrupting their proteolytic processing in infected cells. To test this hypothesis, we labeled HeLa cells infected with Sabin 2, *ABCD* (unmodified prototype), *ABCd* (modified VP1 region), or *abcd* (modified capsid region) with [^{35}S]methionine from 4 to 7 h postinfection and resolved the labeled viral proteins by SDS-PAGE. Unexpectedly, the electrophoretic profiles of the labeled virus-specific proteins were similar for all four viruses, both in the relative intensities of the labeled viral protein bands and in the total amounts of labeled viral proteins produced in the infected cells (Fig. 5A). The four viruses were similar in the efficiency of shutoff of host cell protein synthesis and in the synthesis and processing of viral proteins in infected HeLa cells.

In vitro synthesis of viral proteins in rabbit reticulocytes. The observation that codon replacement had little detectable effect in vivo on viral protein synthesis and processing was mirrored by the results of in vitro translation experiments with rabbit reticulocyte lysates. Full-length in vitro transcripts from cDNA constructs *ABCD*, *ABCd*, and *abcd* programmed the in vitro synthesis and processing of virus-specific proteins with nearly equal efficiencies (Fig. 5B). Taking the results of the in vivo and in vitro protein synthesis experiments together, we found no evidence to support our initial hypothesis that the reduced replicative fitness of the codon replacement viruses was primarily attributable to an impairment of translation and processing of viral proteins.

Specific infectivities of virions of codon replacement viruses. We analyzed the poliovirions produced by HeLa cells infected with viruses *ABCD*, *ABCd*, and *abcd*. Purified infectious virions of all three viruses had similar electrophoretic profiles and the

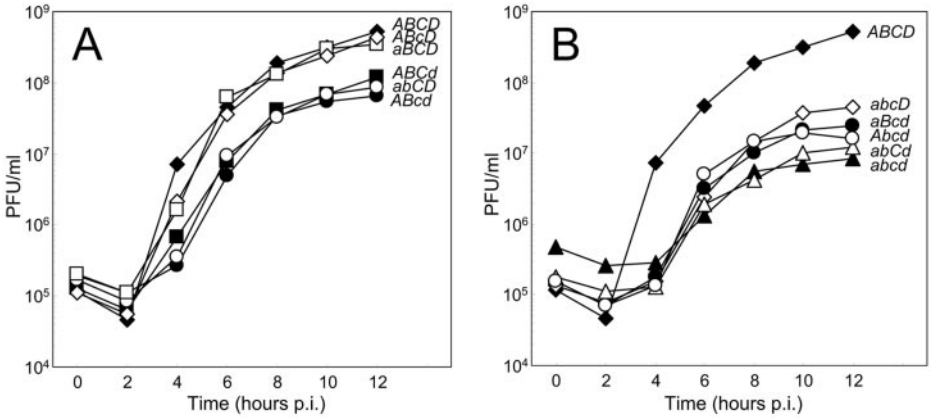

FIG. 4. Growth properties of different virus constructs in single-step growth experiments in HeLa S3 cells at 35°C. Virus constructs with one or two modified cassettes (A) or two to four modified cassettes (B) were compared with the unmodified *ABCD* construct. Single-step growth experiments were performed as described in Materials and Methods, and virus yields were determined by plaque assay on HEp-2C cells (35°C, 72 h). One milliliter of culture contained 4×10^6 HeLa S3 cells.

high VP2/VP0 ratios typical of mature capsids (data not shown). However, the specific infectivities of the purified virions decreased with increased numbers of replacement codons. For example, the particle/PFU ratio increased from 293 (*ABCD*) to 1,221 (*ABCd*) or 5,392 (*abcd*). The magnitude of the decline in specific infectivity was dependent on the choice of infectivity assay and was steeper with the plaque assay than with the limiting dilution assay. This difference arose because the $CCID_{50}$/PFU ratio in HeLa cells increased with the number of replacement codons, from 1.1 (*ABCD*) to 5.4 (*abcd*).

Levels of viral RNA in infected HeLa cells. Alterations in the primary sequence of the viral genome might affect the levels of RNA in infected HeLa cells, either by modifying the rates of RNA synthesis or by changing the stabilities of the intracellular viral RNA molecules. To investigate this possibility, we measured total levels of viral RNA present in infected HeLa cells at 2-h intervals from 0 to 12 h in the single-step growth experiments described above (Fig. 4). Viral RNAs were measured by quantitative PCR, using primers targeting $3D^{pol}$ sequences shared among all viruses. After 12 h, total viral RNA yields were highest (915 ng/ml; equivalent to ~57,000 RNA molecules/cell) for *ABCD*, lower (569 ng/ml; ~35,000 RNA molecules/cell) for *ABCd*, and lowest (330 ng/ml; ~20,000 RNA molecules/cell) for *abcd* (Fig. 6). Plaque yields, in contrast, followed a steeper downward trend, from ~130 PFU/cell (*ABCD*) to ~30 PFU/cell (*ABCd*) and ~2 PFU/cell (*abcd*) (Fig. 3B and 4). Combining these values, we obtained yields of ~440 RNA molecules/PFU (*ABCD*), ~1,200 RNA molecules/PFU (*ABCd*), and ~10,000 RNA molecules/PFU (*abcd*). Although the RNA molecule/PFU ratios were similar to the particle/PFU ratios determined above for each virus, the number of RNA molecules produced in infected cells is typically about twice the number of virus particles, because only about 50% of the viral RNA products are

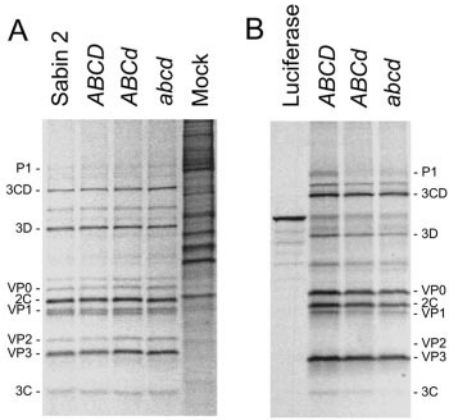

FIG. 5. Poliovirus-specific proteins produced by *ABCD*, *ABCd*, and *abcd* viruses in vivo and in vitro. (A) Lysates of infected HeLa cells (MOI = 25 PFU/cell) labeled with [^{35}S]methionine at 4 to 7 h postinfection. (B) In vitro translation products from rabbit reticulocyte lysates programmed with 250 ng of RNA transcripts from *ABCD*, *ABCd*, and *abcd* cDNAs. Noncapsid proteins were identified by their electrophoretic mobilities and band intensities; capsid proteins were identified by their comigration with proteins from purified virions.

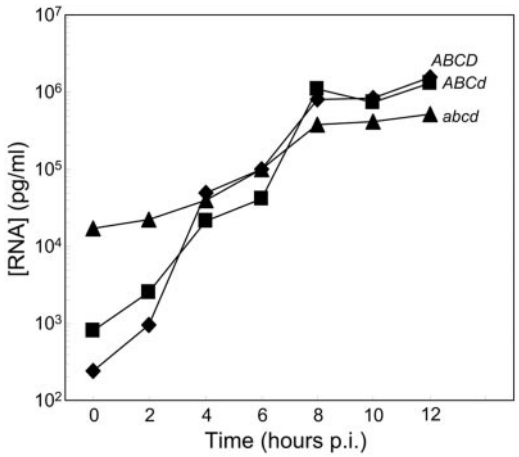

FIG. 6. RNA yields from *ABCD*, *ABCd*, and *abcd* viruses obtained in the single-step growth experiments described in the legend to Fig. 4. RNA levels were determined by quantitative PCRs, using primers and a probe targeting $3D^{pol}$ region sequences that were identical for all three viruses. One picogram of poliovirus RNA corresponds to ~250,000 genomes.

TABLE 3. Nucleotide substitutions in *ABCD*, *ABCd*, and *abcd* viruses during passage in HeLa cells

Virus[a]	nt position	Nucleotide substitution in cells at indicated passage no.											
		RD (1)	HeLa (5)	HeLa (10)	HeLa (15)	HeLa (20)	HeLa (25)	−1 nt[b]	Codon change[c,d]	+4 nt[b]	Amino acid substitution[d]	Gene	Location in polyprotein[e]
ABCD	1439	U	C>U	C	C	C	C	C	C**U**U→C**C**U	G	L→P	VP2	S: NAg-2
	2609	C	C>U	U	U	U	U	U	G**C**A→G**U**A	U	A→V	VP1	I: NC
	3424	U	U>C	C≫U	C	C	C	C	**U**AC→**C**AC	A	Y→H	2A	NC
	3586	A	A	G≫A	G	G	G	G	**A**GA→**G**GA	A	R→G	2A	NC
	5501	A	A	G>A	G	G	G	C	A**A**A→A**G**A	G	K→R	3C	NC
	5630	A	A	A	A>U	U	U	U	C**A**G→C**U**G	G	Q→L	3C	NC
ABCd	1456	A	A≫G	A≫G	A>G	A=G	G>A	U	**A**AC→**G**AC	C	N→D	VP2	S: NAg-2
	2776	A	A	A	A>G	A>G	A>G	G	**A**AG→**G**AG	C	K→E	VP1	S: NAg-1
	2780	G	G≫A	A>G	G>A	G=A	G>A	G	C**G**G↔C**A**G	G	R↔Q	VP1	S: NAg-1
	3120[f]	G	G	G	G>A	A>G≫C	A>C≫G	U	G**C**G→G**C**A	A	A	VP1	I: C
	3377	C	C	C	C>U	C>U	C>U	A	A**C**G↔A**U**G	A	T↔M	VP1	I: NC
	3808	U	U	U	U>C	U>C	U≫C	U	U**A**U→U**G**U	G	Y→R	2A	NC
	3809	A	A>G	G≫A	G=A	G>A	G≫A						
	4350	A	A>G	G>A	G=A	G>A	G=A	C	UUA↔UU**G**	U	L	2C	C
abcd	1169	G	G	G≫A	A≫G	G>A	G>A	G	C**G**G↔C**A**G	A	R↔Q	VP2	I: C
	1447	A	A	A	A	A=G	G>A	G	**A**AC→**G**AC	G	N→D	VP2	S: NAg-2
	1608	U	U	U	U	U=C	C>U	C	G**A**U→G**A**C	A	D	VP2	I: C
	2622	C	C	C≫U	U≫C	C>U	C	C	G**U**C↔G**U**U	G	V	VP1	I: C
	2633	C	C	C	U≫C	C≫U	C	U	G**C**G↔G**U**G	A	A↔V	VP1	I: NC
	2903	A	A	A	A	A=G	G>A	C	**A**AC→**A**GC	U	N→S	VP1	S: NAg-1
	2915	C	C	C>U	C≫U	C>U	C≫U	U	G**C**G↔G**U**G	A	A↔V	VP1	~S: ~NAg-1
	2986	A	A	A	A	A=G	G>A	U	**A**AA→**G**AA	U	K→E	VP1	I: V
	3120[f]	G	G>A	G=A	A≫G	A≫G	A≫G	U	G**C**G→G**C**A	A	A	VP1	I: NC
	3121	A	A	A	A≫C	A>C	A>C	G	**A**AA→**C**AA	G	K→Q	VP1	I: C
	3150	G	G	G	A>G	G	G	C	A**C**G→A**C**A	G	T	VP1	S: NAg-2
	3480	U	U>G	G>U	G≫U	G	G	G	A**G**U→A**G**G	G	S→R	2A	V
	4473	G	G	G	A>G	A	A	C	AA**G**→AA**A**	C	K	2C	C

[a] Virus constructs were as follows: *ABCD*, S2R9; *ABCd*, S2R19; and *abcd*, S2R23.
[b] Nucleotides immediately preceding (−1 nt) and immediately following (+4 nt) the codon.
[c] Each varying nucleotide is shown in boldface type. CG dinucleotides, including those across codons, are underlined.
[d] Rightward-pointing arrows indicate substitutions that steadily accumulated with increased passage numbers; bidirectional arrows indicate bidirectional fluctuations among substitutions.
[e] Locations of amino acid replacements are indicated as follows: S, virion surface residue; NAg, neutralizing antigenic site (41, 48); ~NAg, adjacent to neutralizing antigenic site; I, internal capsid residue not exposed to virion surface; NC, nonconsensus amino acid; V, variable amino acid.
[f] Represents a direct reversion of the engineered codon change.

encapsidated (22). Nonetheless, the two sets of values clearly followed similar trends, as RNA yields and specific virus infectivities declined with increased numbers of replacement codons.

The differences in specific infectivities of the virus particles appear to be largely attributable to differences in the specific infectivities of the viral RNAs. When HeLa monolayers were transfected with equivalent quantities of transcripts from constructs *ABCD*, *ABCd*, and *abcd* and incubated under single-step growth conditions, the relative infectivity yields ($CCID_{50}$; HeLa cells) were 1.0 (*ABCD*), 0.18 (*ABCd*), and 0.016 (*abcd*).

Because the particle/PFU (or RNA molecule/PFU) ratios were higher for the codon replacement viruses than for the unmodified *ABCD* prototype, substantially more *ABCd* and *abcd* virion particles were used to initiate the single-step growth infections, even though the input MOIs varied over a narrow (approximately fourfold) range (Fig. 4). Consequently, the initial input encapsidated RNA levels were high for *ABCd* and very high for *abcd*, such that the extent of amplification of viral RNA at 12 h was ~4,000-fold for *ABCD*, ~1,000-fold for *ABCd*, and only ~20-fold for *abcd* (Fig. 6).

Stabilities of growth phenotypes of codon replacement viruses. We examined the stabilities of the plaque and single-step growth yield phenotypes of the *ABCD*, *ABCd*, and *abcd* viruses during serial passage in HeLa cells. Each virus was passaged 25 times (at 35°C for 36 h) in HeLa cell monolayers, with the input MOI varying from 0.1 to 0.4 PFU/cell; each passage represented at least two infectious cycles. Every fifth passage, virus plaque areas, plaque yields, and the genomic sequences of the bulk virus populations were determined, and the MOI was readjusted to ~0.1 PFU/cell.

All three viruses evolved during serial passage, as measured by increasing plaque sizes, increasing virus yields, and changing genomic sequences (Table 3; Fig. 7). The evolution of the *ABCD* prototype was the least complex. Plaque areas increased approximately sixfold from passage 0 to passage 15, and this was accompanied by nucleotide substitutions at six sites. In contrast, virus yields increased 2.5-fold over the 25 passages. Two substitutions were fixed by passage 10, three more were fixed by passage 15, and all six substitutions were fixed by passage 20 (Table 3). Mixed bases were found at passages 5, 10, and 15. We found no evidence of back mutation or serial substitution at a site. All substitutions mapped to the coding region, and two of the six (33%) mapped to the capsid region, which is close to the proportion of capsid region sequences in the genome (35.4%). In distinct contrast to the pattern of poliovirus evolution in humans, where the large majority of base substitutions generate synonymous codons (43), all six of the observed base substitutions generated amino acid replacements (Table 3). None of the substitutions involved the loss of a CG dinucleotide.

The evolution of the codon replacement constructs was much more complex and dynamic. In *ABCd*, four of the eight (50%) variable positions mapped to VP1 (12.1% of the genome), and three of these four mapped within codon replacement cassette *d* (9.2% of the genome) (Table 3). Substitutions at half of the positions involved the apparent loss of CG

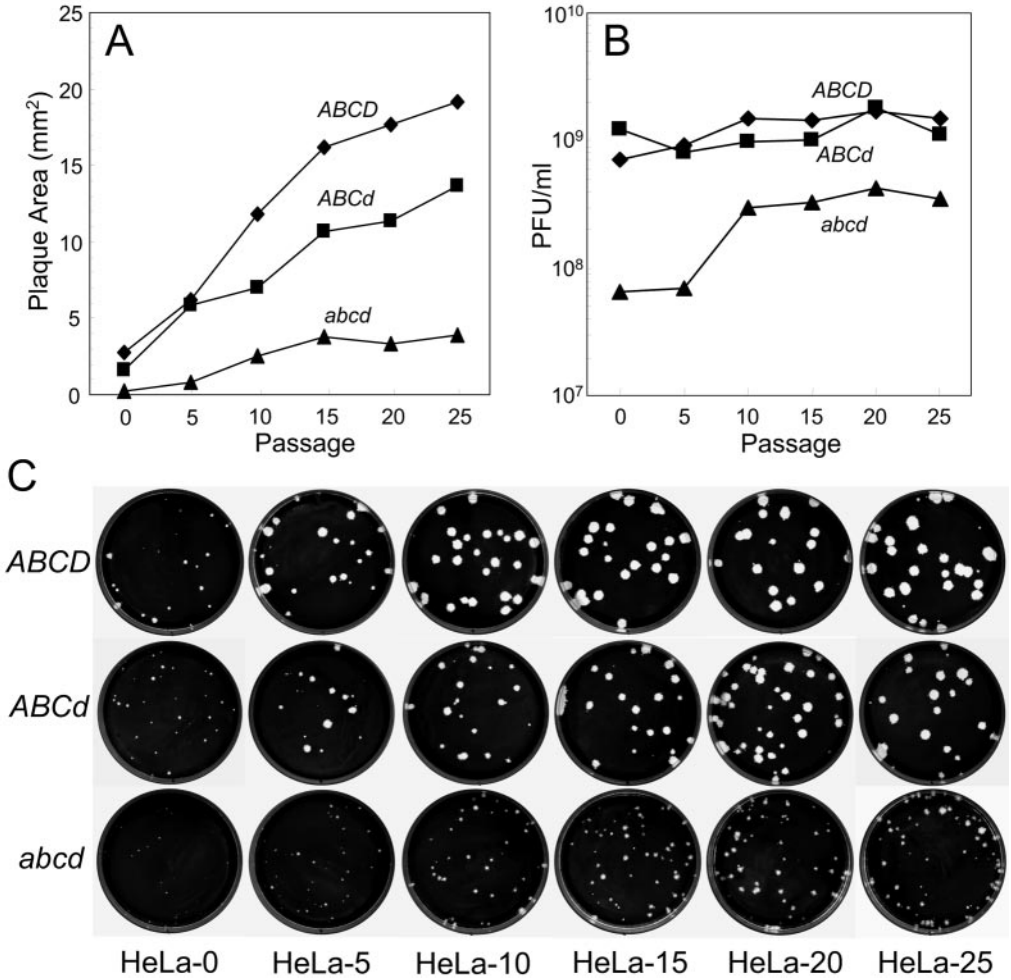

FIG. 7. Virus passage in HeLa monolayer cells at 35°C. (A) Mean plaque areas of evolving viruses were determined by plaque assay on HeLa cells (35°C, 60 h). (B) Virus titers were determined by plaque assay on HeLa cells at 35°C on every fifth passage. (C) Plaque morphologies on HeLa cells (35°C, 60 h).

dinucleotides (6.3% of the total genome), although in all instances the loss from the virus population was incomplete. One cassette *d* substitution (G_{3120}→A) eliminating a CG dinucleotide represented a back mutation to the original synonymous codon. Virus *ABCd* resembled the *ABCD* prototype in that six of the eight nucleotide substitutions generated amino acid replacements. In contrast, *ABCd* differed markedly from the *ABCD* prototype in other ways, as the dynamics of substitution had apparently not stabilized by passage 25, and mixed bases were found at all eight positions of variability (Table 3). Active sequence evolution was accompanied by progressively increasing plaque areas over an approximately sixfold range, while virus yields fluctuated over a narrower, approximately twofold range (Fig. 7).

The evolution of *abcd* was the most dynamic, as determined by expanding plaque areas, rising virus yields, and increasing numbers of observed nucleotide substitutions. Plaque areas increased ~15-fold from passage 0 to passage 15 and then stabilized (Fig. 7). Virus yields increased most sharply (approximately fourfold) between passages 5 and 10 but remained approximately fourfold lower than those of *ABCD* and *ABCd* at passage 25 (Fig. 7B). Among the 13 sites of nucleotide variability, most (11/13; 84.6%) mapped to the capsid region, all within the codon replacement interval; eight mapped within the VP1 region, three mapped within the VP2 region, and none mapped within the VP3 region (Table 3). As with the other constructs, most (8/13; 61.5%) of the substitutions encoded amino acid replacements. Substitutions at six sites involved a partial, transient, or complete loss of CG dinucleotides. As in *ABCd*, a G_{3120}→A substitution eliminated a CG dinucleotide and restored the original Sabin 2 base. This same reversion was observed in eight other independent passages of *abcd* virus (data not shown). The two variable sites outside the capsid region stabilized with new substitutions by HeLa cell passage 20, whereas 8 of the 11 variable sites within the capsid region still had mixed bases at passage 25. Interestingly, no substitutions were found in the $3D^{pol}$ region, even though it constitutes 26% of the total genome. Apart from the back mutation at position 3120, all other variable sites differed between *ABCD*, *ABCd*, and *abcd*. No net changes were observed at sites A_{481} (in the 5′ UTR) and U_{2909} (in the VP1 region), which are known to be subject to strong negative selection

when Sabin 2 replicates in the human intestine (44, 49, 78, 79), and no changes were found at other sites known to vary upon propagation of Sabin 2 in cell culture (69).

In addition to the elimination of several CG dinucleotides, there was also a net loss (one lost, five partially lost, and one gained) of UA dinucleotides in the high-passage isolates (Table 3). In the codon replacement constructs, the elimination of UA dinucleotides was incomplete up to passage 25. Most (four of six) UA losses involved amino acid replacements. Unlike codons most frequently associated with a loss of CG dinucleotides, none of the codons associated with a loss of UA dinucleotides were replacement codons. While not as strongly suppressed as CG dinucleotides, UA dinucleotides are underrepresented in poliovirus genomes (61, 70) and human genes (34).

Most (8 of 13) of the capsid amino acid replacements mapped within or near surface determinants forming neutralizing antigenic (NAg) sites (Table 3). Although surface determinants are generally the most variable (70), amino acid replacements also occurred in naturally variable nonsurface residues in VP1 (Lys→Glu) and $2A^{pro}$ (Ser→Arg). Most of the synonymous mutations mapped to codons for conserved amino acids. However, several of the amino acid replacements, including five of the six in *ABCD*, were mutations to nonconsensus residues (Table 3).

Sequence evolution in HeLa cells of the unmodified *ABCD* virus differed in important respects from that of the codon replacement *ABCd* and *abcd* viruses. Nucleotide substitutions in the *ABCD* progeny were dispersed across the ORF, dimorphic variants emerged in the early passages, all six mutations were fixed by passage 20, and a single dominant master sequence emerged. In contrast, populations of the *ABCd* and *abcd* progeny were complex mixtures of variants at least up to passage 25, and the majority base at the variable sites typically fluctuated from passage to passage. Apparently, the incorporation of nonpreferred codons into the *ABCd* and *abcd* genomes led to an expansion of the mutant spectrum (14) and to the emergence of complex and unstable quasispecies populations. Because we have not attempted to isolate separate variants from the mixed populations, we do not know the phenotypes of individual sequence variants within the quasispecies.

Predicted RNA secondary structures of codon replacement virus genomes. The genomic RNAs of polioviruses and other enteroviruses appear to have relaxed secondary structures outside the 5′ UTR, the 3′ UTR, and the *cis*-acting replication element (CRE) within the 2C region (54, 73). Accordingly, under physiological conditions, most bases within the ORF can pair with more than one partner, and poliovirus genomes can fold into many different secondary structures having similar thermodynamic stabilities (54). However, the incorporation of numerous base substitutions into the codon replacement constructs and the concomitant increase in G+C content might destabilize folding patterns that had been subject to natural selection and stabilize other pairings absent from the unmodified Sabin 2 genome. To investigate the effects of codon replacement on RNA folding patterns, we compared the predicted secondary structures of the complete genomes of *ABCD*, *ABCd*, and *abcd* calculated using the mfold v. 3.1 algorithm (47, 54, 73, 82). The calculated global thermodynamic stabilities (expressed as minimum free energies at 35°C [$\Delta G_{35°C}$], or MinE) of the RNA secondary structures increased with increasing G+C contents (for *ABCD*, $\Delta G_{35°C} = -2{,}047$ kcal/mol; for *ABCd*, $\Delta G_{35°C} = -2{,}078$ kcal/mol; and for *abcd*, $\Delta G_{35°C} = -2{,}191$ kcal/mol), and the number of predicted stem structures increased from 546 (*ABCD*) to 557 (*ABCd*) and 562 (*abcd*). Much of the increased thermodynamic stability of the *abcd* RNA is attributable to more extensive folding within the P1/capsid region. Because the in vivo pairings are likely to be flexible and dynamic, many suboptimal structures are predicted to have nearly equivalent thermodynamic stabilities to those of the MinE structures (47, 54, 82). When the suboptimal structures ($\Delta\Delta G_{35°C}$ of up to +12 kcal/mol) were considered, the *abcd* RNA was again predicted to have a higher likelihood of folding within the P1/capsid region than the *ABCD* and *ABCd* RNAs. It is difficult to assess rigorously the structural contributions of the nucleotide substitutions that accumulated during serial passage of the *ABCd* and *abcd* viruses because the final progeny were mixed populations. However, when we analyzed the majority base sequence for each final passage population, the calculated MinE values and the numbers of stem structures were similar between each pair of parental and progeny RNAs. Moreover, the higher-fitness *abcd* progeny was predicted to have retained the tendency for increased folding in the P1/capsid region. Although some preferred short-range and long-range pairings varied among the different RNAs, the stable secondary structures in the 5′ UTR, the 3′ UTR, and the CRE were predicted to be unaltered.

DISCUSSION

Replacement of the original capsid region codons of the Sabin 2 OPV strain with synonymous nonpreferred codons resulted in sharp reductions in virus replicative fitness in HeLa cells. The reductions in fitness, as measured by plaque areas and virus yields, were approximately proportional to the numbers of replacement codons. Plaque areas were reduced ~90% and virus yields were reduced >98% in the *abcd* virus, in which the replacement interval spanned nearly the entire capsid region. The observed fitness declines in the codon replacement viruses cannot be attributed to amino acid substitutions because all viral genomes encoded the same reference Sabin 2 polyprotein sequence.

The inverse relationship between replicative fitness and the number of codon replacements suggests that the observed phenotypes are the cumulative effects of numerous nucleotide substitutions. However, the contributions of individual replacement codons or of the nine different categories of codon replacements are presently unknown. We attempted to identify the most critical codon replacements by monitoring which substitutions accumulated in the genomes of codon replacement viruses upon serial passage in HeLa cells. Only one substitution, G_{3120}→A, a direct back mutation to the original sequence, was shared between derivatives of the *ABCd* and *abcd* viruses after serial passage. The 19 other independent substitutions found among the *ABCd* and *abcd* high-passage derivatives were associated with 12 different codon triplets. Codon replacement in the VP1 region appeared to have proportionately greater effects on replicative fitness than replacements in other capsid intervals, an observation reinforced by the finding that 8 of the 13 sites that varied upon serial passage of *abcd* mapped to the VP1 region. Replacement of VP1 region codons in the genome of the unrelated wild poliovirus type 2 prototype

strain, MEF-1, also appeared to have a disproportionately high impact on growth (R. Campagnoli, unpublished results).

Multiple synonymous capsid codon replacements appear necessary to effect any discernible reductions in poliovirus fitness. In our initial experiments, replacement of 3 to 14 Arg codons in VP1 (0.3% to 1.6% of capsid codons) with CGG (among the least preferred codons in the poliovirus genome) (61, 70) did not result in any apparent reduction in plaque areas. The requirement for multiple codon replacements for evident impairment of gene expression is consistent with the effects of codon replacements in the phosphoglycerate kinase gene of yeast (23) and in the L1 and L2 capsid protein genes of bovine papillomavirus (81). In contrast, the introduction of small numbers (1, 6, and 10) of strongly nonpreferred CUA Leu codons into the 5′ region of the alcohol dehydrogenase gene of *Drosophila* did result in significant reductions in enzyme activity (10). Our ability to detect small declines in poliovirus fitness might be improved by replacing the plaque assay, which invariably gives heterogeneous plaques, with a more consistent biochemical assay. The major advantage of the plaque assay and the other virus infectivity assays used in this study is their high sensitivities to very low levels of biological activity.

The underlying biological mechanisms controlling the observed fitness reductions in the codon replacement viruses are not well defined. By analogy with bacterial (4), yeast (23), insect (10), and viral (81) systems, we had originally hypothesized that reliance on a restricted set of nonpreferred codons for the synthesis of capsid region polypeptides might cause a local depletion of the pools of minor tRNAs, thus retarding translocation of the ribosome along the viral mRNA. Ribosomal pausing at nonpreferred codons might impair poliovirus protein synthesis and processing in various ways, such as by amino acid misincorporation (55), by increasing the costs of translational proofreading (9), by frameshifting (18), by premature polypeptide chain termination (55), by degradation of the RNA template (23), and by disruption of the proteolytic processing of the polyprotein (56). On the other hand, it has been suggested that the nonrandom locations of nonpreferred codons between structural elements may facilitate proper folding of the nascent capsid proteins of poliovirus (19) and hepatitis A virus (66). However, we did not detect any major alterations in vivo or in vitro in the synthesis and processing of the viral proteins of the codon replacement viruses. It is possible that more direct measurements of the rates of polypeptide chain elongation, the dynamics of protein folding, or the kinetics of protein processing might reveal differences not evident from the initial experiments described here.

One possible explanation for our results is that poliovirus RNA is not equivalent to a highly expressed gene, as it is not translated as efficiently as mRNAs of the most highly expressed mammalian genes. Polypeptide chain elongation rates are ~220 amino acids per min for poliovirus in HeLa cells at 37°C (58), compared with ~600 amino acids per min for the α chain of hemoglobin in rabbit reticulocytes (25). Moreover, some codons rarely used in poliovirus genomes are frequently used in highly expressed mammalian genes, such that the levels of the tRNAs for these codons may be high and therefore difficult to deplete.

The pattern of reversion among high-passage progeny of the codon replacement virus constructs suggests that increased numbers of CG dinucleotides may contribute to reductions in fitness. Our strategy for codon replacement raised the number of CG dinucleotides in the poliovirus complete ORF from 181 (*ABCD*) to 386 (*abcd*). Although the biological basis for CG suppression in RNA viruses is poorly understood (33), selection against CG dinucleotides during serial passage of *ABCd* and *abcd* appeared to be sufficiently strong at some sites to drive amino acid substitutions in the normally well-conserved poliovirus capsid proteins. In every instance, CG suppression was incomplete and was frequently reversed upon further passage. The most stable trends toward CG suppression involved nucleotide positions 3120 and 3150 and were not associated with amino acid changes.

The maintenance of a flexible mRNA secondary structure has been suggested to be a possible factor for codon selection (16, 21, 23, 33). The increased G+C contents of our constructs, which were higher than those found in any known natural poliovirus templates, might impede translocation of the ribosome by favoring the formation of new highly stable stem structures. However, the increased fitness of the *ABCD*, *ABCd*, and *abcd* progenies after serial passage was not associated with any predicted decreases in RNA secondary structure. Poliovirus genomes are evidently capable of accommodating abrupt shifts in the potential pairing structures within the ORF, as would likely occur following natural recombination events (42, 77). It remains unknown whether perturbations in RNA secondary structure contribute in any way to the observed reductions in virus replicative fitness.

The observation that the eclipse phases in the single-step growth experiments were increasingly prolonged as the number of replacement codons increased suggests that codon replacement viruses were less efficient at completing an early step (or steps), following attachment and uncoating, of the infectious cycle. This view is reinforced by the observation that the specific infectivities of the virus particles and the RNA transcripts decreased sharply with the number of replacement codons. It thus appears that a larger number of codon replacement virus particles (and genome equivalents) is required to initiate a replicative cycle but that once the cycle has started, the synthesis and processing of viral proteins are nearly normal. Although the total viral RNA yield was reduced only ~3-fold in the most highly modified *abcd* virus, its viral RNA amplification was only ~20-fold, suggesting that an impairment of viral RNA synthesis may contribute to reduced replicative fitness.

Despite our incomplete understanding of the underlying biological mechanisms, it may yet be possible to refine our basic strategy for fitness modulation in poliovirus. Additional (e.g., AUA [Ile], AAA [Lys], and CAU [His]) and redesigned (e.g., UCG [Ser]) codon substitutions that are better matched to the least abundant tRNA genes in the human genome (28) may further reduce replicative fitness. It is also possible to incorporate an additional 159 CG dinucleotides across capsid region codons without altering the encoded amino acid sequences. Targeting codons for conserved amino acids may further stabilize the reduced fitness phenotype, as most pathways for phenotypic reversion would likely favor synonymous substitutions only. If nonpreferred codons at strategic sites facilitate proper folding of capsid proteins (19, 66), then their replacement with preferred codons might further reduce fitness. In the absence of a clear

understanding of the molecular mechanisms, the approach toward minimizing replicative fitness by the replacement of capsid region codons remains empirical and may involve tradeoffs between different mechanisms. It is important that the most highly modified virus, *abcd*, with an infectious yield of <10 PFU/cell in both HEp-2C and HeLa cells, already appears to be near the threshold of viability. Therefore, the margin for further fitness reductions may be quite narrow, although it may still be possible to obtain improvements in phenotypic stabilities.

The systematic modulation of RNA virus replicative fitness by deoptimization of codon usage may have applications for producing RNA viruses having well-defined replicative properties. If, as we suggest, the observed fitness reductions in the codon replacement viruses are the cumulative effects of multiple substitutions whose individual selection coefficients for reversion are small (10), then full phenotypic reversion may require numerous mutational steps occurring over many replication cycles. Such viruses would likely be much more stable than most RNA virus point mutants (72) and could lead to the development of live, attenuated RNA virus vaccines with superior genetic stabilities.

ACKNOWLEDGMENTS

We thank Qi Chen and Jane Iber for investigating some of the growth properties of the codon replacement strains, A. J. Williams and Naomi Dybdahl-Sissoko for characterizing the antigenic properties of the strains, and Brian Holloway and Melissa Olsen-Rasmussen for preparing the synthetic deoxyoligonucleotides used in this study.

The findings and conclusions in this report are those of the authors and do not necessarily represent the views of the funding agency.

REFERENCES

1. **Akashi, H.** 2001. Gene expression and molecular evolution. Curr. Opin. Genet. Dev. **11:**660–666.
2. **Akashi, H., and A. Eyre-Walker.** 1998. Translational selection and molecular evolution. Curr. Opin. Genet. Dev. **8:**688–693.
3. **André, S., B. Seed, J. Eberle, W. Schraut, A. Bültmann, and J. Haas.** 1998. Increased immune response elicited by DNA vaccination with a synthetic gp120 sequence with optimized codon usage. J. Virol. **72:**1497–1503.
4. **Barak, Z., D. Lindsley, and J. Gallant.** 1996. On the mechanism of leftward frameshifting at several hungry codons. J. Mol. Biol. **256:**676–684.
5. **Bennetzen, J., and B. Hall.** 1982. Codon selection in yeast. J. Biol. Chem. **257:**3026–3031.
6. **Brown, B. A., and E. Ehrenfeld.** 1980. Initiation factor preparations from poliovirus-infected cells restrict translation in reticulocyte lysates. Virology **103:**327–339.
7. **Brown, B. A., and E. Ehrenfeld.** 1979. Translation of poliovirus RNA in vitro: changes in cleavage pattern and initiation sites by ribosomal salt wash. Virology **97:**396–405.
8. **Brown, B. A., M. S. Oberste, K. Maher, and M. Pallansch.** 2003. Complete genomic sequencing shows that polioviruses and members of human enterovirus species C are closely related in the non-capsid coding region. J. Virol. **77:**8973–8984.
9. **Bulmer, M.** 1991. The selection-mutation-drift theory of synonymous codon usage. Genetics **129:**897–907.
10. **Carlini, D. B., and W. Stephan.** 2003. In vivo introduction of unpreferred synonymous codons into the Drosophila Adh gene results in reduced levels of ADH protein. Genetics **163:**239–243.
11. **Chen, T. R.** 1988. Re-evaluation of HeLa, HeLa S3, and HEp-2 karyotypes. Cytogenet. Cell Genet. **48:**19–24.
12. **Chiapello, H., F. Lisacek, M. Caboche, and A. Henaut.** 1998. Codon usage and gene function are related in sequences of Arabidopsis thaliana. Gene **209:**GC1–GC38.
13. **Chumakov, K. M.** 1996. PCR engineering of viral quasispecies: a new method to preserve and manipulate genetic diversity of RNA virus populations. J. Virol. **70:**7331–7334.
14. **Domingo, E., E. Baranowski, C. Escarmís, F. Sobrino, and J. J. Holland.** 2002. Error frequencies of picornavirus RNA polymerases: evolutionary implications for virus populations, p. 285–298. *In* B. L. Semler and E. Wimmer (ed.), Molecular biology of picornaviruses. ASM Press, Washington, D.C.
15. **Dominguez, G., C. Y. Wang, and T. K. Frey.** 1990. Sequence of the genome RNA of rubella virus: evidence for genetic rearrangement during togavirus evolution. Virology **177:**225–238.
16. **Duret, L.** 2002. Evolution of synonymous codon usage in metazoans. Curr. Opin. Genet. Dev. **12:**640–649.
17. **Estes, M. K.** 2001. Rotaviruses and their replication, p. 1747–1785. *In* D. M. Knipe, P. M. Howley, D. E. Griffin, R. A. Lamb, M. A. Martin, B. Roizman, and S. E. Straus (ed.), Fields virology, 4th ed. Lippincott Williams & Wilkins, Philadelphia, Pa.
18. **Gallant, J., P. Bonthuis, and D. Lindsley.** 2003. Evidence that the bypassing ribosome travels through the coding gap. Proc. Natl. Acad. Sci. USA **100:**13430–13435.
19. **Gavrilin, G. V., E. A. Cherkasova, G. Y. Lipskaya, O. M. Kew, and V. I. Agol.** 2000. Evolution of circulating wild poliovirus and of vaccine-derived poliovirus in an immunodeficient patient: a unifying model. J. Virol. **74:**7381–7390.
20. **Georgescu, M. M., F. Delpeyroux, and R. Crainic.** 1995. Tripartite genome organization of a natural type 2 vaccine/nonvaccine recombinant poliovirus. J. Gen. Virol. **76:**2343–2348.
21. **Hartl, D. L., E. N. Moriyama, and S. A. Sawyer.** 1994. Selection intensity for codon bias. Genetics **138:**227–234.
22. **Hewlett, M. J., S. Rozenblatt, V. Ambros, and D. Baltimore.** 1977. Separation and quantitation of intracellular forms of poliovirus RNA by agarose gel electrophoresis. Biochemistry **16:**2763–2767.
23. **Hoekema, A., R. A. Kastelein, M. Vasser, and H. A. de Boer.** 1987. Codon replacement in the *PGK1* gene of *Saccharomyces cerevisiae*: experimental approach to study the role of biased codon usage in gene expression. Mol. Cell. Biol. **7:**2914–2924.
24. **Hughes, P. J., D. M. Evans, P. D. Minor, G. C. Schild, J. W. Almond, and G. Stanway.** 1986. The nucleotide sequence of a type 3 poliovirus isolated during a recent outbreak of poliomyelitis in Finland. J. Gen. Virol. **67:**2093–2102.
25. **Hunt, T., T. Hunter, and A. Munro.** 1969. Control of haemoglobin synthesis: rate of translation of the messenger RNA for the alpha and beta chains. J. Mol. Biol. **43:**123–133.
26. **Ikemura, T.** 1981. Correlation between the abundance of *Escherichia coli* transfer RNAs and the occurrence of the respective codons in its protein genes. J. Mol. Biol. **146:**1–21.
27. **Ikemura, T.** 1982. Correlation between the abundance of yeast transfer RNAs and the occurrence of the respective codons in protein genes. Differences in synonymous codon choice patterns of yeast and *Escherichia coli* with reference to the abundance of isoaccepting transfer RNAs. J. Mol. Biol. **158:**573–597.
28. **International Human Genome Sequencing Consortium.** 2001. Initial sequencing and analysis of the human genome. Nature **409:**860–921.
29. **Jenkins, G. M., and E. C. Holmes.** 2003. The extent of codon usage bias in human RNA viruses and its evolutionary origin. Virus Res. **92:**1–7.
30. **Kanaya, S., Y. Yamada, M. Kinouchi, Y. Kudo, and T. Ikemura.** 2001. Codon usage and tRNA genes in eukaryotes: correlation of codon usage diversity with translation efficiency and with CG-dinucleotide usage as assessed by multivariate analysis. J. Mol. Evol. **53:**290–298.
31. **Kane, J. F.** 1995. Effects of rare codon clusters on high-level expression of heterologous proteins in Escherichia coli. Curr. Opin. Biotechnol. **6:**494–500.
32. **Kärber, G.** 1931. Beitrag zur kollektiven Behandlung pharmakologischer Reihenversuche. Arch. Exp. Pathol. Pharmakol. **162:**480–483.
33. **Karlin, S., W. Doerfler, and L. R. Cardon.** 1994. Why is CpG suppressed in the genomes of virtually all small eukaryotic viruses but not in those of large eukaryotic viruses? J. Virol. **68:**2889–2897.
34. **Karlin, S., and J. Mrázek.** 1996. What drives codon choices in human genes? J. Mol. Biol. **262:**459–472.
35. **Kew, O. M., V. Morris-Glasgow, M. Landaverde, C. Burns, J. Shaw, Z. Garib, J. André, E. Blackman, C. J. Freeman, J. Jorba, R. Sutter, G. Tambini, L. Venczel, C. Pedreira, F. Laender, H. Shimizu, T. Yoneyama, T. Miyamura, H. van der Avoort, M. S. Oberste, D. Kilpatrick, S. Cochi, M. Pallansch, and C. deQuadros.** 2002. Outbreak of poliomyelitis in Hispaniola associated with circulating type 1 vaccine-derived poliovirus. Science **296:**356–359.
36. **Kitamura, N., B. L. Semler, P. G. Rothberg, G. R. Larsen, C. J. Adler, A. J. Dorner, E. Emini, R. Hanecak, J. J. Lee, S. van der Werf, C. W. Anderson, and E. Wimmer.** 1981. Primary structure, gene organization and polypeptide expression of poliovirus RNA. Nature **291:**547–553.
37. **Kohara, M., T. Omata, T. Kameda, B. L. Semler, H. Itoh, E. Wimmer, and A. Nomoto.** 1985. In vitro phenotypic markers of a poliovirus recombinant constructed from infectious cDNA clones of the neurovirulent Mahoney strain and the attenuated Sabin 1 strain. J. Virol. **53:**786–792.
38. **Laemmli, U. K.** 1970. Cleavage of structural proteins during the assembly of the head of bacteriophage T4. Nature **227:**680–685.
39. **La Monica, N., C. Meriam, and V. R. Racaniello.** 1986. Mapping of sequences required for mouse neurovirulence of poliovirus type 2 Lansing. J. Virol. **57:**515–525.
40. **Lehrach, H., D. Diamond, J. M. Wozney, and H. Boedtker.** 1977. RNA molecular weight determinations by gel electrophoresis under denaturing conditions, a critical reexamination. Biochemistry **16:**4743–4751.

41. **Lentz, K. N., A. D. Smith, S. C. Geisler, S. Cox, P. Buontempo, A. Skelton, J. DeMartino, E. Rozhon, J. Schwartz, V. Girijavallabhan, J. O'Connell, and E. Arnold.** 1997. Structure of poliovirus type 2 Lansing complexed with antiviral agent SCH48973: comparison of the structural and biological properties of three poliovirus serotypes. Structure **5:**961–978.
42. **Liu, H.-M., D.-P. Zheng, L.-B. Zhang, M. S. Oberste, O. M. Kew, and M. A. Pallansch.** 2003. Serial recombination during circulation of type 1 wild-vaccine recombinant polioviruses in China. J. Virol. **77:**10994–11005.
43. **Liu, H.-M., D.-P. Zheng, L.-B. Zhang, M. S. Oberste, M. A. Pallansch, and O. M. Kew.** 2000. Molecular evolution of a type 1 wild-vaccine poliovirus recombinant during widespread circulation in China. J. Virol. **74:**11153–11161.
44. **Macadam, A. J., S. R. Pollard, G. Ferguson, R. Skuce, D. Wood, J. W. Almond, and P. D. Minor.** 1993. Genetic basis of attenuation of the Sabin type 2 vaccine strain of poliovirus in primates. Virology **192:**18–26.
45. **Martín, J., G. Dunn, R. Hull, V. Patel, and P. D. Minor.** 2000. Evolution of the Sabin strain of type 3 poliovirus in an immunodeficient patient during the entire 637-day period of virus excretion. J. Virol. **74:**3001–3010.
46. **Martín, J., G. L. Ferguson, D. J. Wood, and P. D. Minor.** 2000. The vaccine origin of the 1968 epidemic of type 3 poliomyelitis in Poland. Virology **278:**42–49.
47. **Mathews, D. H., J. Sabina, M. Zuker, and D. H. Turner.** 1999. Expanded sequence dependence of thermodynamic parameters improves prediction of RNA secondary structure. J. Mol. Biol. **288:**911–940.
48. **Minor, P. D.** 1990. Antigenic structure of picornaviruses. Curr. Top. Microbiol. Immunol. **161:**121–154.
49. **Minor, P. D., and G. Dunn.** 1988. The effect of sequences in the 5′ noncoding region on the replication of polioviruses in the human gut. J. Gen. Virol. **69:**1091–1096.
50. **Moriyama, E. N., and J. Powell.** 1997. Codon usage bias and tRNA abundance in *Drosophila*. J. Mol. Evol. **45:**514–523.
51. **Musto, H., S. Cruvellier, G. D'Onofrio, H. Romero, and G. Bernardi.** 2001. Translational selection on codon usage in *Xenopus laevis*. Mol. Biol. Evol. **18:**1703–1707.
52. **Nottay, B. K., O. M. Kew, M. H. Hatch, J. T. Heyward, and J. F. Obijeski.** 1981. Molecular variation of type 1 vaccine-related and wild polioviruses during replication in humans. Virology **108:**405–423.
53. **Osawa, S., T. H. Jukes, K. Watanabe, and A. Muto.** 1992. Recent evidence for evolution of the genetic code. Microbiol. Rev. **56:**229–264.
54. **Palmenberg, A. C., and J.-Y. Sgro.** 1997. Topological organization of picornaviral genomes: statistical prediction of RNA structural signals. Semin. Virol. **8:**231–241.
55. **Parker, J.** 1989. Errors and alternatives in reading the universal genetic code. Microbiol. Rev. **53:**273–298.
56. **Racaniello, V. R.** 2001. *Picornaviridae*: the viruses and their replication, p. 685–722. *In* D. M. Knipe, P. M. Howley, D. E. Griffin, R. A. Lamb, M. A. Martin, B. Roizman, and S. E. Straus (ed.), Fields virology, 4th ed. Lippincott Williams & Wilkins, Philadelphia, Pa.
57. **Racaniello, V. R., and D. Baltimore.** 1981. Molecular cloning of poliovirus cDNA and determination of the complete nucleotide sequence of the viral genome. Proc. Natl. Acad. Sci. USA **78:**4887–4891.
58. **Rekosh, D.** 1972. Gene order of the poliovirus capsid proteins. J. Virol. **9:**479–487.
59. **Rezapkin, G. V., L. Fan, D. M. Asher, M. R. Fibi, E. M. Dragunsky, and K. M. Chumakov.** 1999. Mutations in Sabin 2 strain of poliovirus and stability of attenuated phenotype. Virology **258:**152–160.
60. **Robinson, M., R. Lilley, S. Little, J. S. Emtage, G. Yarronton, P. Stephens, A. Millican, M. Eaton, and G. Humphreys.** 1984. Codon usage can affect efficiency of translation of genes in *Escherichia coli*. Nucleic Acids Res. **12:**6663–6671.
61. **Rothberg, P. G., and E. Wimmer.** 1981. Mononucleotide and dinucleotide frequencies, and codon usage in poliovirion RNA. Nucleic Acids Res. **9:**6221–6229.
62. **Rueckert, R. R.** 1976. On the structure and morphogenesis of picornaviruses, p. 131–213. *In* H. Fraenkel-Conrat and R. R. Wagner (ed.), Comprehensive virology, vol. 6. Plenum Press, New York, N.Y.
63. **Rueckert, R. R., and M. A. Pallansch.** 1981. Preparation and characterization of encephalomyocarditis (EMC) virus. Methods Enzymol. **78:**315–325.
64. **Sabin, A. B., and L. R. Boulger.** 1973. History of Sabin attenuated poliovirus oral live vaccine strains. J. Biol. Stand. **1:**115–118.
65. **Sambrook, J., and D. W. Russell.** 2001. Molecular cloning: a laboratory manual, 3rd ed. Cold Spring Harbor Laboratory Press, Cold Spring Harbor, N.Y.
66. **Sánchez, G., A. Bosch, and R. M. Pintó.** 2003. Genome variability and capsid structural constraints of hepatitis A virus. J. Virol. **77:**452–459.
67. **Smith, D. W.** 1996. Problems of translating heterologous genes in expression systems: the role of tRNA. Biotechnol. Prog. **12:**417–422.
68. **Stemmer, W. P. C., A. Crameri, K. D. Ha, T. M. Brennan, and H. L. Heyneker.** 1995. Single-step assembly of a gene and entire plasmid from large numbers of oligodeoxyribonucleotides. Gene **164:**49–53.
69. **Taffs, R. E., K. M. Chumakov, G. V. Rezapkin, Z. Lu, M. Douthitt, E. M. Dragunsky, and I. S. Levenbook.** 1995. Genetic stability and mutant selection in Sabin 2 strain of oral poliovirus vaccine grown under different cell culture conditions. Virology **209:**366–373.
70. **Toyoda, H., M. M. Kohara, Y. Kataoka, T. Suganuma, T. Omata, N. Imura, and A. Nomoto.** 1984. Complete nucleotide sequences of all three poliovirus serotype genomes: implication for genetic relationship, gene function and antigenic determinants. J. Mol. Biol. **174:**561–585.
71. **Urrutia, A. O., and L. D. Hurst.** 2001. Codon usage bias covaries with expression breadth and the rate of synonymous evolution in humans, but this is not evidence for selection. Genetics **159:**1191–1199.
72. **Wimmer, E., C. U. Hellen, and X. Cao.** 1993. Genetics of poliovirus. Annu. Rev. Genet. **27:**353–436.
73. **Witwer, C., S. Rauscher, I. L. Hofacker, and P. F. Stadler.** 2001. Conserved RNA secondary structures in *Picornaviridae* genomes. Nucleic Acids Res. **29:**5079–5089.
74. **Wright, F.** 1990. The effective number of codons used in a gene. Gene **87:**23–29.
75. **Xia, X.** 1998. How optimized is the translational machinery in *Escherichia coli*, *Salmonella typhimurium*, and *Saccharomyces cerevisiae*? Genetics **149:**37–44.
76. **Yadava, A., and C. F. Ockenhouse.** 2003. Effect of codon optimization on expression levels of a functionally folded malaria vaccine candidate in prokaryotic and eukaryotic expression systems. Infect. Immun. **71:**4961–4969.
77. **Yang, C.-F., H.-Y. Chen, J. Jorba, H.-C. Sun, S.-J. Yang, H.-C. Lee, Y.-C. Huang, T.-Y. Lin, P.-J. Chen, H. Shimizu, Y. Nishimura, A. Utama, M. Pallansch, T. Miyamura, O. Kew, and J.-Y. Yang.** 2005. Intratypic recombination among lineages of type 1 vaccine-derived poliovirus emerging during chronic infection of an immunodeficient patient. J. Virol. **79:**12623–12634.
78. **Yang, C.-F., T. Naguib, S.-J. Yang, E. Nasr, J. Jorba, N. Ahmed, R. Campagnoli, H. van der Avoort, H. Shimizu, T. Yoneyama, T. Miyamura, M. A. Pallansch, and O. Kew.** 2003. Circulation of endemic type 2 vaccine-derived poliovirus in Egypt, 1983 to 1993. J. Virol. **77:**8366–8377.
79. **Yoshida, H., H. Horie, K. Matsuura, T. Kitamura, S. Hashizume, and T. Miyamura.** 2002. Prevalence of vaccine-derived polioviruses in the environment. J. Gen. Virol. **83:**1107–1111.
80. **Ypma-Wong, M. F., and B. L. Semler.** 1987. In vitro molecular genetics as a tool for determining the differential cleavage specificities of the poliovirus 3C proteinase. Nucleic Acids Res. **15:**2069–2088.
81. **Zhou, J., W. J. Liu, S. W. Peng, X. Y. Sun, and I. Frazer.** 1999. Papillomavirus capsid protein expression level depends on the match between codon usage and tRNA availability. J. Virol. **73:**4972–4982.
82. **Zuker, M., D. H. Matthews, and D. H. Turner.** 1999. Algorithms and thermodynamics for RNA secondary structure prediction: a practical guide, p. 1–23. *In* J. Barciszewski and B. F. C. Clark (ed.), RNA biochemistry and biotechnology. Kluwer Academic Publishers, Norwell, Mass.